Launch Acoustics of the Falcon 9 Rocket: Source Characteristics and Models

Logan T. Mathews

A senior thesis submitted to the faculty of
Brigham Young University
in partial fulfillment of the requirements for the degree of

Bachelor of Science

Kent L. Gee, Advisor

Department of Physics and Astronomy

Brigham Young University

ABSTRACT

Launch Acoustics of the Falcon 9 Rocket: Source Characteristics and Models

Logan T. Mathews
Department of Physics and Astronomy, BYU
Bachelor of Science

This study investigates the source characteristics of the Falcon 9 rocket from a series of measurements and evaluates models for maximum overall level, directivity, and radiated sound power. These models are based on a handful of rocket parameters and provide a basic description these rocket source characteristics. The models for maximum level and sound power perform well, while the angle of maximum radiation falls between historic predictions for static and launched vehicles.

Keywords: rocket noise, directivity, sound power, jet noise, Falcon 9

ACKNOWLEDGMENTS

I would like to thank Kent Gee and Grant Hart for their contributions to this research and my education. Kent got me into physics in the first place and has mentored me through my education and research, providing opportunities to learn, teach, and contribute to the scientific community.

To my my fellow research students- you contributed to measurements, reviewed and revised my writing, and made research both interesting and fun. You helped me learn that science is best approached as a collaborative effort- not a personal foray. Thanks for bringing great ideas and good times!

I would also like to thank those in my family who have supported me through my education, particularly my wife Bryn. Her contributions to my education and life are bar none. Thanks, Bryn, for being my number one supporter and for always seeking the adventure in life!

Contents

List of Figures

List of Tables

Chapter 1

Introduction

1.1 Motivation

Understanding the acoustic characteristics of space launch vehicles is increasingly important as launch trends continue to rise (as seen in Fig. 1.1) and more launch facilities are built. Increases in both the number of launches and the number of spaceports worldwide will create a greater environmental and human impact. In order to address the impacts of rocket noise, an accurate understanding of the noise generated by rockets is imperative. Although many studies were performed from the mid 1950's through the 1970's, there remains the need for additional studies to reconcile historical differences and better inform the jet noise community on the source characteristics of large rockets. While many source characteristics have been examined, directivity, peak level, and radiated sound power are fundamental to the understanding of launch vehicle noise. Simple models for predicing launch vehicle acoustics can inform important decisions regarding rocket and spaceport development.

This thesis is organized as follows: first, a brief discussion of the source of jet noise is given. Second, an overview of the state of rocket noise research in the literature is given. In the measurement chapter, the details of the measurement and launch vehicle are given with

important discussion on uncertainty, meteorology, and related factors. The analysis chapter contains findings from the Falcon 9 and comparisons with historical source models. The research documented in this thesis is analyzed and discussed more comprehensively in two publications in the literature, Mathews et al. (2020) [1] and Mathews et al. (2021) [2].

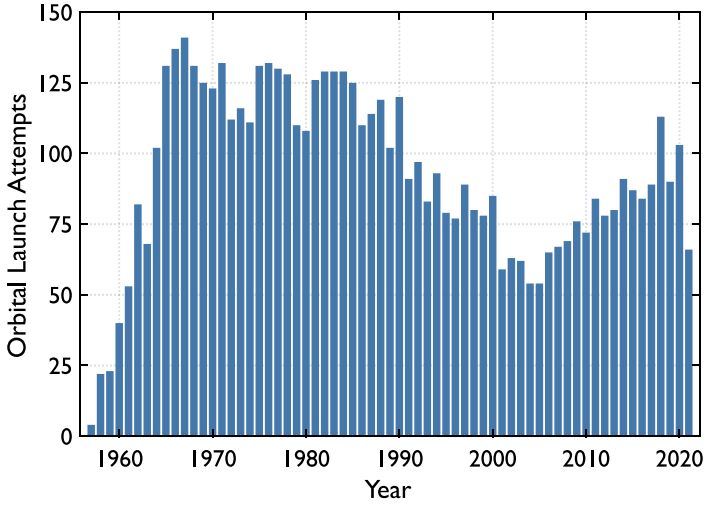

Figure 1.1 Orbital rocket launch trends from 1957-present. Although launches peaked in the 1960's and then delcined, recently a resurgent trend has occurred as launches have become cheaper and more avaliable.

1.2 Background

1.2.1 Jet Noise and Mechanisms of Sound Generation

To understand jet noise is to understand both the meaning of the term and the mechanism whereby noise is created by a jet. A jet is a directed stream of fluid flowing out of a nozzle or other orifice. Jet noise, then, is the noise generated by this fluid flow situation. Of particular interest in this study is supersonic jet noise, or the noise generated by a jet whose velocity is faster than the speed of sound.

In a rocket, exhaust gases are expelled at a supersonic velocity (U_e). While the flow is generally smooth immediately after the nozzle, this smooth flow maintained for only a few jet exit diameters (D_e) downstream. As the stream of gas meets the static atmosphere, the transition between supersonic flow and static atmosphere forms a shear layer between the two fluid regions. Due to the extreme velocity difference at the boundary, the shear layer is unstable and turbulent structures, or eddies, are formed in this layer and grow as Kelvin-Helmholtz instabilities. These turbulent structures do not stay in place, however, as they are convected downstream by the local mean flow. The supersonic gases in the rocket exhaust "push" these eddies downstream. The approximate convective speed of these large turbulent structures is typically represented by a convective Mach number M_c. An illustration of this is given in Fig. 1.2. This convective movement of turbulent structures is not entirely unlike an aircraft moving at a supersonic velocity. The aircraft (or turbulent structure) disturbs the surrounding atmosphere, which when moving faster than the speed of sound produces a sonic boom (or better referred to as Mach waves with the case of supersonic turbulent structures in a jet). Thus, in summary: supersonic gases exiting the rocket meet with the static atmosphere and form a turbulent shear layer, whose turbulent structures are convected downstream at a supersonic speed, creating directional mach wave radiation, as illustrated in Fig. 1.2.

A regular Mach number can be associated with a supersonic aircraft, and the resulting angle of the sonic boom can be predicted using the formulation

$$\theta = \cos^{-1} \frac{1}{M}. \tag{1.1}$$

Considering our analogous example in context of jet turbulence, the angle of Mach wave radiation could be readily predicted if the velocity at which the turbulence is convected could be found. However, the speed of convecting turbulence (usually represented as a convective Mach number, M_c) is a rather complex and nuanced problem. No analytical solutions exist for this convective speed due to the randomness of turbulence. Many experiments have come up

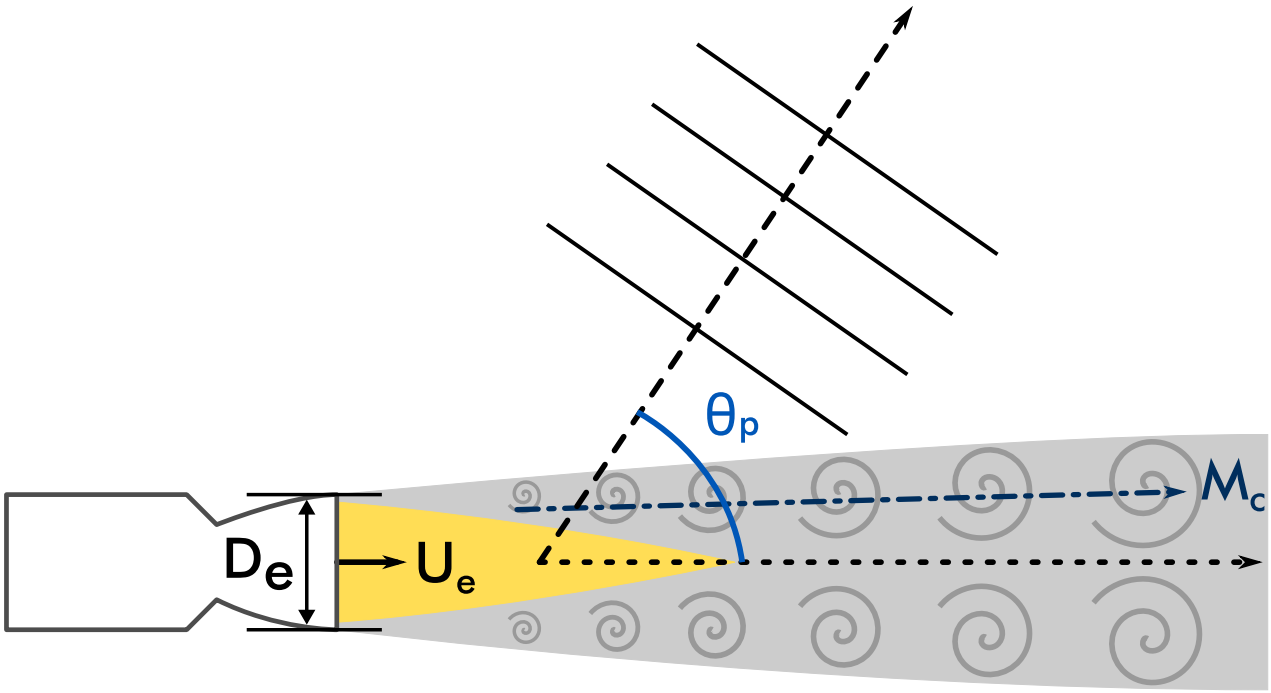

Figure 1.2 Representation of a rocket plume with turbulent structures producing directional Mach wave radiation

with reasonable approximations for the average convective speed of these turbulent structures, though. In the literature, many studies place the speed somewhere between 60% and 80% of the jet centerline velocity (this percentage is typically represented by the symbol κ). Alternative empirical formulations were given by Oertel [3], who classified observed turbulent structures into three categories, each with a distinct velocity given in Eqs. (1.2), (1.3), and (1.4).

$$M_c = \frac{U_j}{c_j + c_a} \tag{1.2}$$

$$M_c' = \frac{U_j + c_j}{c_j + c_a} \tag{1.3}$$

$$M_c'' = \frac{U_j - c_j}{c_j + c_a} \tag{1.4}$$

1.2.2 Historical Studies

Levels

One of the most fundamental characteristics of acoustics is the amplitude of sound. Sound is simply a pressure disturbance in a medium. As common sound pressures in air span nine orders of magnitude, compressing these sound pressures into sound pressure levels (SPL) using the decibel quantity allows nine orders of magnitude to be compressed to just three. The sound pressure level across all frequencies is referred to as the overall sound pressure level (OASPL). The OASPLs associated with rocket launches allow a basic quantification of rocket noise. When measured and predicted accurately, these data can inform policy on noise generation, impacts, and mitigation procedures. Among these studies, Cole and Thomas [4] provide a basic overview of the far-field levels of a Saturn launch. More recently, Putnicki [5] has provided a more extensive and detailed survey of far-field noise levels from a Space Shuttle launch. Putnicki [5] attempts to use a previous static fire to model the launch noise at different distances, but finds that the modeled levels are about 10 dB(A) lower than measured for the launch. The findings in this study do indicate azimuthal symmetry of radiation, which is useful in the determination of overall sound power from measurements.

Directivity

Any source of sound that has a directional radiation pattern can be described with a directivity. The directivity pattern shows how energy is radiated into surrounding space. As previously discussed, the primary, far-field contribution to jet noise is Mach wave radiation. Since Mach wave radiation is directional, the parameters of the rocket flow are connected to the angle at which noise is radiated.

The directivity associated with rocket noise is extensively studied, but significant discrepancies exist between reported directivity patterns. In addition, differences in directivity have also been

observed between horizontally fired static rockets and launched rockets. One of the earliest observations of this was made by Cole *et al.* [6] who notes that peak radiation differs 20° on average between static and launched rockets. McInerny [7] notes this discrepancy and suggests horizontally fired static rocket directivities may be affected by ground effects not present in launch vehicle measurements. Other studies have such as Mayes *et al.* [8] and Potter and Crocker [9] find similar directivities for static rockets. Sutherland [10] investigates the static and launch directivities of similar large rockets and finds the static and launched directivities to differ by 10°.

Sound Power

Sound power encompasses the total acoustic energy that is emitted by a source of sound. Neglecting other effects such as absorption, the sound power is independent of distance or geometry. Many proposed methods of estimating rocket sound power have been proposed; possibly the most widespread involves sound being radiated as a proportion of the mechanical power of the rocket. Eldred [11], Guest [12], and Sutherland [10] have all considered a 0.5% radiation efficiency for large rockets to be reasonable, with Eldred [11] considering 1% radiation efficiency to be a conserative upper bound.

1.2.3 Modern Studies

Levels

Greska *et al.* [13] have proposed a model connecting peak level scaled to 100 equivalent exit diameters ($D_{e,\text{equiv}} = D_e\sqrt{N}$ where N is the number of nozzles) with a convective Mach number characteristic of the plume.This connection with a convective Mach number directly connects a predicted level to the physical properties of the plume, and promises an easy estimation of levels with just the rocket parameters alone.

In addition to Greska's model, McInerny [7] proposed a power-based prediction method for

OASPL in the direction of maximum radation.

Directivity

Based on an early measurement by Kenny *et al.* [14], James *et al.* [15] have examined the directivity for a horizontally fired static Reusable Shuttle Rocket Motor (RSRM) and predicted the peak radiation angle to be around 64° relative to the exit axis of the rocket. This value falls between historical predictions for static and launched rockets. With regards to launched vehicles, however, very few directivities have been published in the last four decades due to the relative scarcity of published rocket trajectory information.

1.3 Purpose

The purpose of this paper is to establish basic source characteristics for the Falcon 9 rocket and to evaluate historical models for source characteristics. Accomplishing these provides better understanding of how noise is radiated from rockets and how models can be used to understand and predict rocket noise. The verification of models allows for basic acoustic predctions of a broad category of launch vehicle noise based on a handful of parameters, without need for costly simulations or extensive measurements.

Chapter 2

Methods

2.1 Measurement

2.1.1 Location

The dataset used in this study contains acoustical measurements of three launches of the Falcon 9 rocket from Vandenberg Space Force Base (VAFB), California. All three launches originated from the same launch facility, SLC-5E. Vandenberg is located near the community of Lompoc on the coast of the Pacific Ocean. Between the inland community of Lompoc and the costal launch facility at VAFB lies a large area of open fields where the majority of measurements were conducted. Additionally, south of the Lompoc community lies San Miguelito canyon where an additional measurement location was placed for one launch.

The three measured launches involved the same launch vehicle and although the payload and trajectories varied by launch, the variability is relatively minor, especially in the first 100 seconds of launch where the trajectory is primarily vertical.

Four primary measurement locations were used, referred to as North Field (NF), West Field (NF), East Field (EF), and Miguelito Canyon (MC), although only the NF location remained at

a consistent location across launches. A map of the locations relative to the launch site and community of Lompoc is given in Fig. 2.1. These locations varied radially between 7 km and 13 km from the launch facility. A summary of each of these locations is given in Table 2.1.

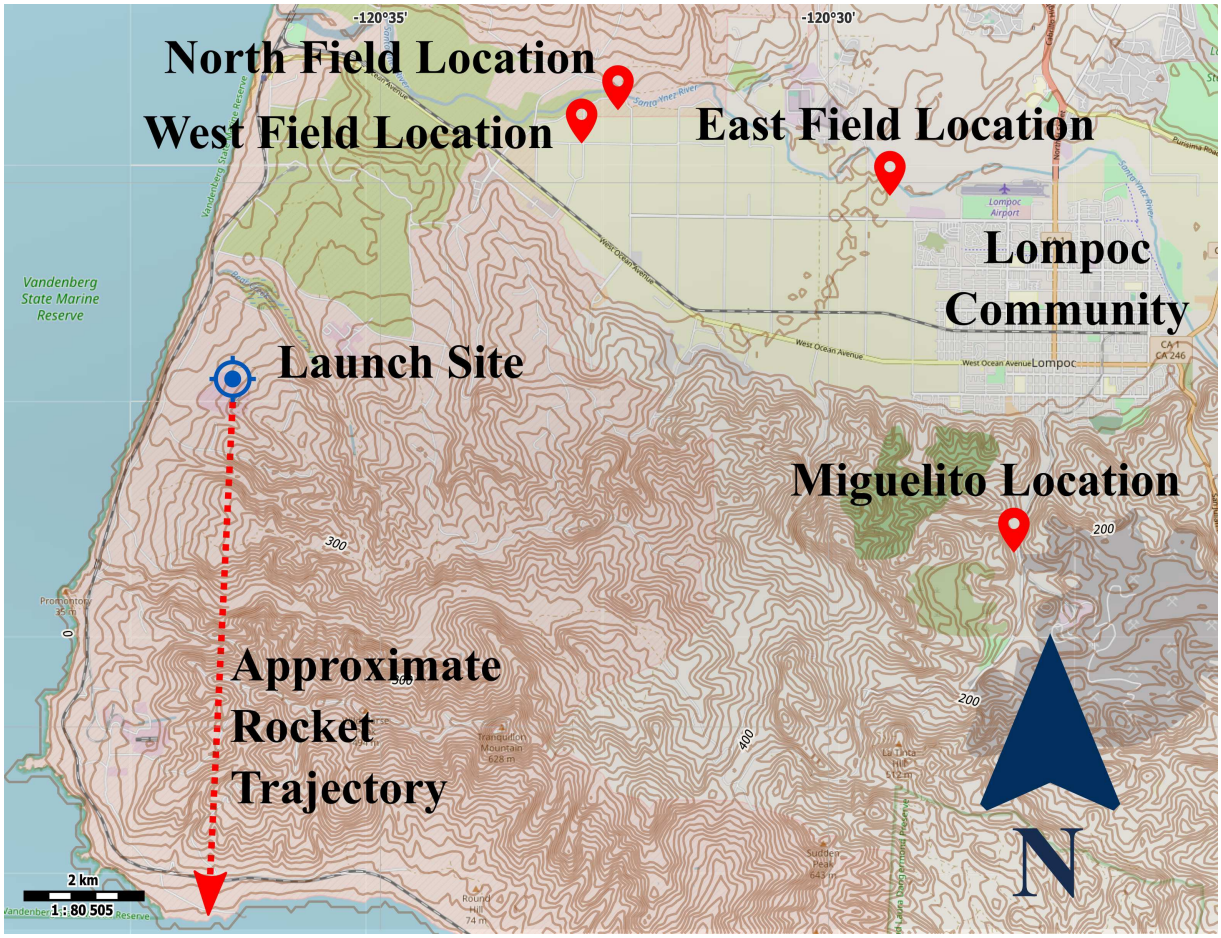

Figure 2.1 Map of the measurement layout for the launch measurements. The North, East, and West Field locations all lie within a flat field area. The East Field and Miguelito locations are unique to the RADARSAT Constellation launch.

All of the locations exhibit some form of terrain shielding for the earliest portions of the launch, as seen from the elevation profiles in Fig. 2.2. All of the field locations have similar elevation profiles, while the Miguelito location lies in a canyon with significantly more complex terrain between the launch facility and the measurement location. Effects of terrain shielding will

Location	Launches	Radius, m	Heading re Launch Complex
West Field (WF)	I7N, S1A, RC	6565-7758	$50 - 53°$
North Field (NF)	I7N, S1A, RC	8208-8345	$50 - 51°$
East Field (EF)	RC	11388	$72°$
Miguelito Canyon (MC)	RC	13685	$100°$

Table 2.1 Details for each of the measurement locations. Location varied the greatest between launches for the West Field location. The North Field location was kept as consistent as possible between all three launches.

be investigated at this location.

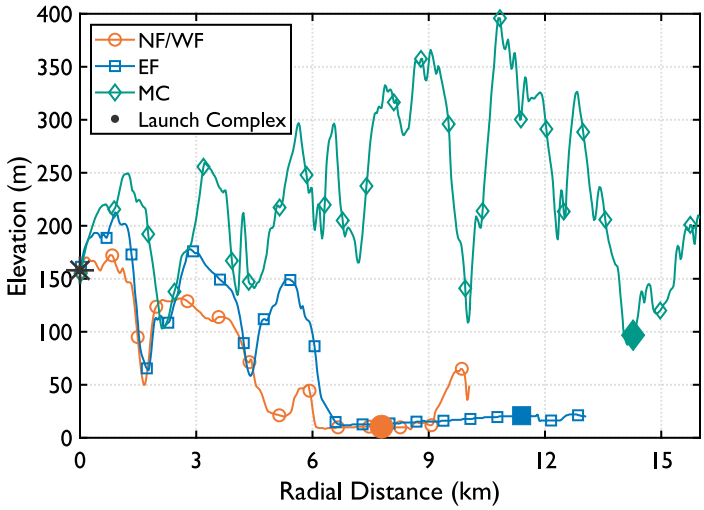

Figure 2.2 Elevation Profiles for North/West Field, East Field, and Miguelito locations. Measurement locations are indicated by filled-in markers.

2.1.2 Launch Vehicle

The Falcon 9 launch vehicle is an orbital class, partially reusable, medium- to heavy-lift launch vehicle. It has quickly grown to be one of the most frequently launched rockets in the United States, with 26 launches in 2020 and 45 launches planned for 2021. The Falcon 9 is a two-stage

liquid fueled rocket. The first stage is comprised of a group of nine Merlin 1D engines, while the second stage is powered by a single vacuum-optimized Merlin engine. Each engine is fueled by a combination of RP-1 and LOX, common rocket fuels. At sea level, each one of the nine Merlin engines produces a maximum thrust of 845 kN, amounting for a total maximum first stage thrust of 7.6 MN at sea level. A table of estimated engine parameters for the Falcon 9 rocket is given in Table 2.3.

2.1.3 Instrumentation

Given that peak frequencies for rocket noise are predominantly infrasonic ($f < 20$ Hz), low frequency capable measurement equipment is used to accurately measure low frequencies. Good low frequency instrumentation response is key to the analysis of rocket waveforms and time-domain statistics, as shown by McInerny *et al.* [16]. Measurement systems were based upon the BYU-developed Portable Unit for Measuring Acoustics (PUMA) architecture [17], utilizing National Instruments® CompactDAQ (cDAQ) data acquisition hardware.

While a variety of microphone types and configurations were used across the measurements, a consistent low-frequency capable setup was used at each location. This consisted of a PCB 378A07 or GRAS 47AC microphone and a Compact Unit for Ground-based Acoustical Recordings (COUGAR), a low profile configuration with high wind noise rejection that minimizes ground reflection interference (development and performance of the COUGAR apparatus is reported by Gee *et al.* [18]). Low-frequency cutoff tolerances for the data acquisition equipment used is given in Table 2.2. Figure 2.3 shows a deployed data acquisition system (referred to as a portable unit for measuring acoustics or PUMA) at the North Field location for the S1A launch.

Type	Model	Low Frequency Cutoff	Tolerance
Microphone	PCB 378A07	0.13 Hz	±2 dB
Microphone	GRAS 47AC	1 Hz	±1 dB
cDAQ Module	NI 9234	0.5 Hz	±2 dB
cDAQ Module	NI 9250	0.43 Hz	±3 dB

Table 2.2 Low frequency cutoff specifications for data acquisition hardware used

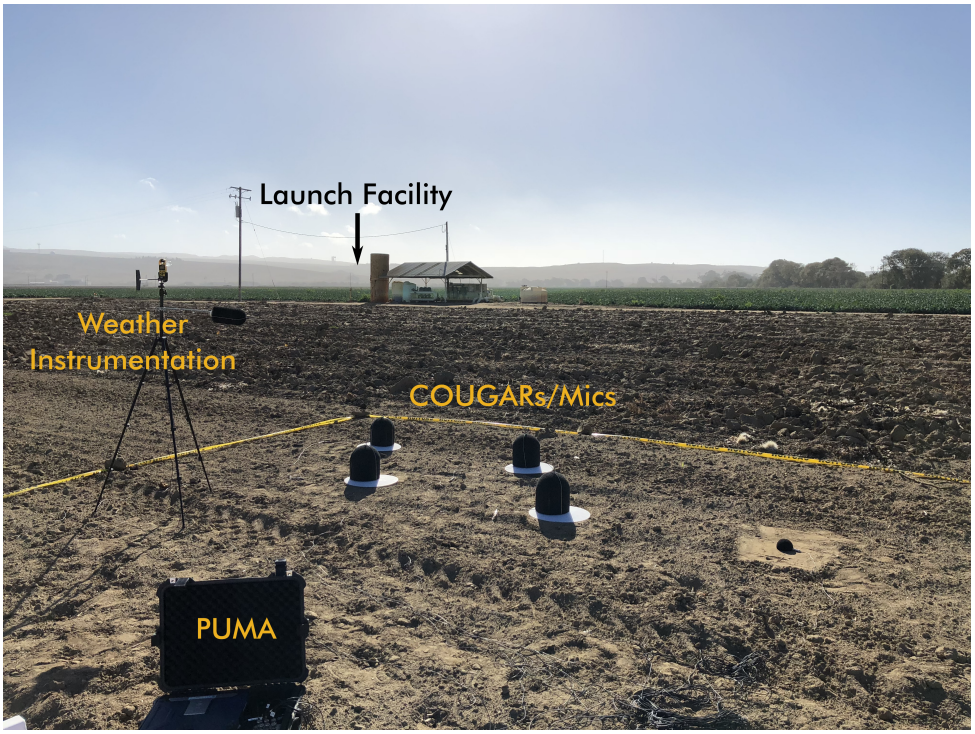

Figure 2.3 North Field measurement location for S1A launch. The launch facility lies over the hills in the distance as indicated.

2.2 Analysis Methods

2.2.1 Propagation Speed and Temporal Uncertainty

For all analyses, an assumed mean propagation speed of 340 m/s is used. As the altitude of the source varies, the sound speed will also vary due to temperature and atmospheric winds. Effective sound speed profiles for each launch at one location and all locations at the RC launch are calculated from radiosonde data collected the same day as each launch and are shown in Fig. 2.4. While this effective sound speed profile shows variation with altitude, most of the analyses in this study are confined to altitudes below 5 km. From this, the mean propagation speed is within $\pm$10 m/s, and is less than than that when averaged for the I7 and RC launches. The sound speed profile varies greater with the S1A launch likely due to this measurement occurring in the evening with clear skies in the fall, as opposed to the other two occurring during summer mornings with dense fog. Peak directivity is achieved with the rocket below 4 km in altitude, so the sound speed profiles for all three launches are reasonably close in this region, though.

To distance correct amplitudes during the launch, the $\pm$10 m/s variability in sound speed would result in an amplitude correction error less than 1 dB, which a sufficient level of accuracy for the analyses considered.

2.2.2 Time

Upon ignition, rocket engines produce an ignition overpressure (IOP) that is observable as a low-frequency impulse in the waveform. As each measurement location is not absolutely synchronized with the other locations and the rocket, the IOP is used to time synchronize each measurement. This time alignment is verified using a crosscorrelation to validate that the datasets are aligned accurately, within $\pm$ 1 ms.

Due to propagation, there is a time scale discrepancy between the measurement locations

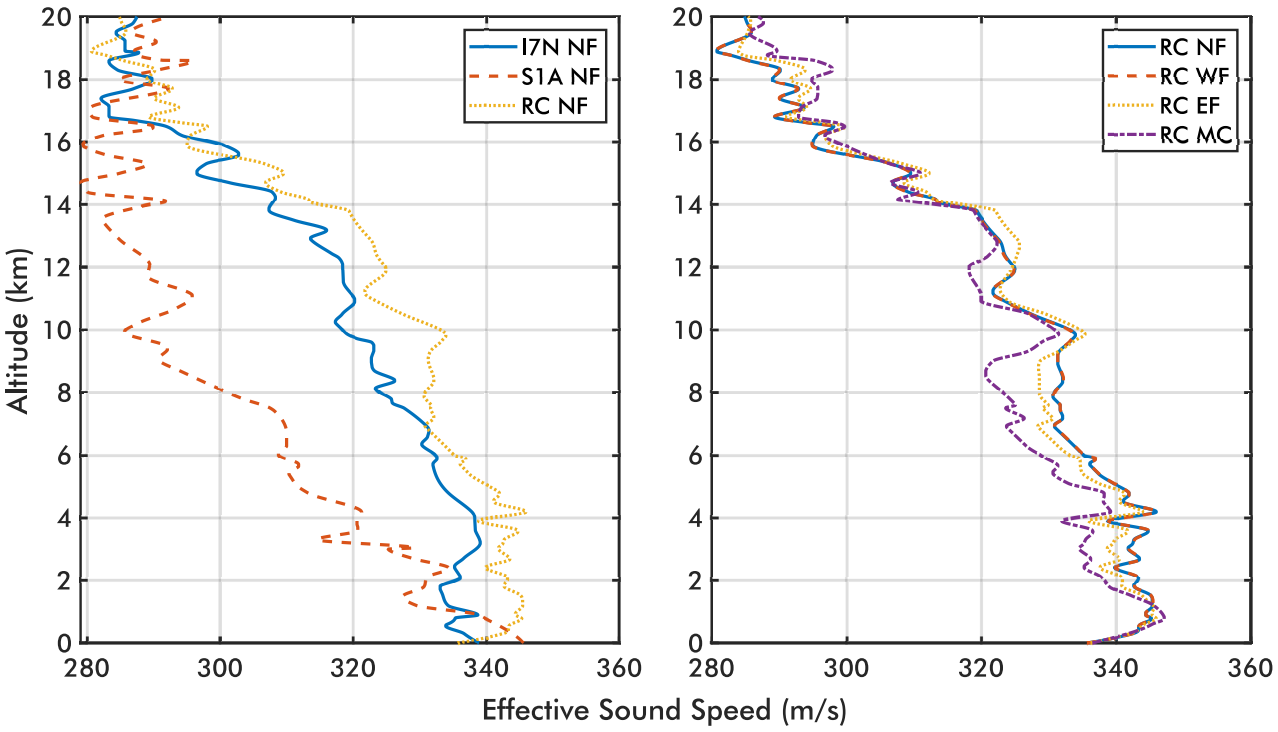

Figure 2.4 Effective soundspeed profiles for (a) each launch at the North Field (NF) location and (b) each measurement location at the RADARSAT Constellation (RC) launch. Temperature and windspeed are considered.

and the rocket itself. When referencing time, generally observer time is used. In the early stages of the launch, the difference in observer time between stations is accounted for by the tine alignment of the data; as the rocket increases in altitude, the propagation path difference between the locations becomes less significant.

2.2.3 Scaling for Geometric Spreading

Since sites at different radii are being compared, correcting amplitudes for geometric spreading becomes necessary. Typically, a correction for atmospheric absorption would also be included in distance correction. However, due to the high amplitude of the noise measured, nonlinear propagation reduces the effects of atmospheric absorption. Nonlinear propagation results in

wave steepening, a phenomenon where the noise becomes more shock-like resulting in an increase of high frequencies which offsets the greater attenuation of higher frequencies due to absorption/thermoviscous losses. Thus, only geometric spreading will be considered in correcting for propagation distance. Some analyses, such as those performed by McInerny *et al.* [19] include absorptive effects, however, this analysis will not. In order to perform level corrections, trajectory information is used to determine the straight-ray propagation distances from the rocket to the measurement locations. The trajectory information is considered to be accurate to within 10 percent, which results in level correction accuracy of ± 1 dB.

2.3 Ideal Expansion

For a jet, optimal exit conditions are achieved when the exit pressure (P_e) of the jet is equal to the pressure of the surrounding atmosphere (P_a). Given that rocket engines operate across a wide variety of altitudes (and therefore pressures), the ideal condition will not always be achieved. The result is over- and under-expansion of the jet when ambient pressures are greater than or less than the exit pressure of the jet, respectively. Overexpansion of the jet results in a "pinching" of the flow inwards, and results in flow separation before the exit of the nozzle due to the formation of oblique shocks. Conversely, when the ambient pressure is less than than the exit pressure, the jet operates at an underexpanded condition, and the flow "balloons" out immediately after leaving the nozzle. A visualization of these conditions is shown in Fig. 2.5.

Two principal numerical theories exist for estimating rocket flow characteristics: frozen and equilibrium flow. The frozen flow case assumes that any chemical reactions cease when the gas leaves the combustion chamber (from the narrow neck in Fig 2.5 onwards), thus the ratio of specific heats downstream is a quasi-constant (i.e. the chemical composition of the gasses does not change significantly with distance). The chemical equilibrium case assumes that reactions continue to occur, rapidly enough to adjust to the near instantaneous changes in temperature and

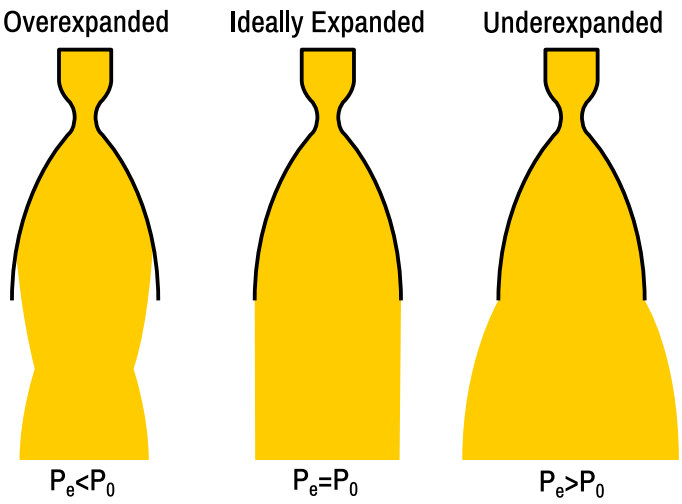

Figure 2.5 Illustration of overexpanded, ideally expanded, and underexpanded nozzle conditions.

pressure. It must be noted that both methods produce reasonably accurate estimates of rocket parameters; however neither are ultimately accurate in their description of rocket combustion, which is a very complex compressible flow problem. While there is a matter of debate over which theory is most accurate, both are considered to be reasonably accurate.

Using the NASA Chemical Equilibrium Program CEA2, we obtained the following exit parameters in Table 2.3 using equilibrium flow.

T_e	exit temperature	1786 K
T_j	fully-expanded exit temperatue	1879 K
P_e	exit pressure	75.8 kPa
P_j	fully-expanded exit pressure	101 kPa
c_e	exit sound speed	876 m/s
c_j	fully-expanded exit sound speed	898 m/s
U_e	exit velocity	3092 m/s
U_j	fully-expanded exit veloctiy	3029 m/s
M_e	exit Mach number	3.531
M_j	fully-expanded exit Mach number	3.377
γ_e	ratio of specific heats at exit	2098 K
D_e	exit diameter	0.92 m
D_j	fully-expanded diameter	0.83 m
$D_{e,\text{equiv.}}$	equivalent diameter for all 9 engines	2.76 m
D_t	throat diameter	0.23 m
Th	sea-level thrust, each engine	845 kN

Table 2.3 Various parameters for the exit jet of the Falcon 9 rocket's Merlin 1D engines for a chamber pressure of 10.8 MPa assuming equilibrium flow.

Chapter 3

Results and Conclusions

3.0.1 Representative Falcon 9 Data

A representative waveform from the RADARSAT Constellation launch, West Field location, is shown in Fig. 3.1. Half-second waveform excerpts are also shown for four different time periods during the launch. These correspond to the ignition overpressure, peak directivity, mid-launch, and late-launch periods, respectively. The ignition overpressure is readily observable at t = 0 s in Fig. 3.1(a) as a low-frequency impulse. The period of the impulse is greater than that observed with other measured ignition overpressures shown by Ryan *et al.* [20]. High acoustic shock content is visible at peak directivity around t = 42 s in Fig. 3.1(b). Figure 3.1(c) shows continued acoustic shock content at t = 100 s, but with reduced amplitude and lower overall frequency content. Figure 3.1(d) shows an even more exaggerated reduction in amplitude and increase in high frequency content at t = 300 s. Even with the attenuation present in Fig. 3.1(d), there are very clear and pronounced acoustic shocks present. Considering that the waveform observed at 300 s was generated nearly 65 km distant, the presence of such pronounced shock structures is of note.

Figure 3.2 shows the running OASPL and spectra from various periods of the launch

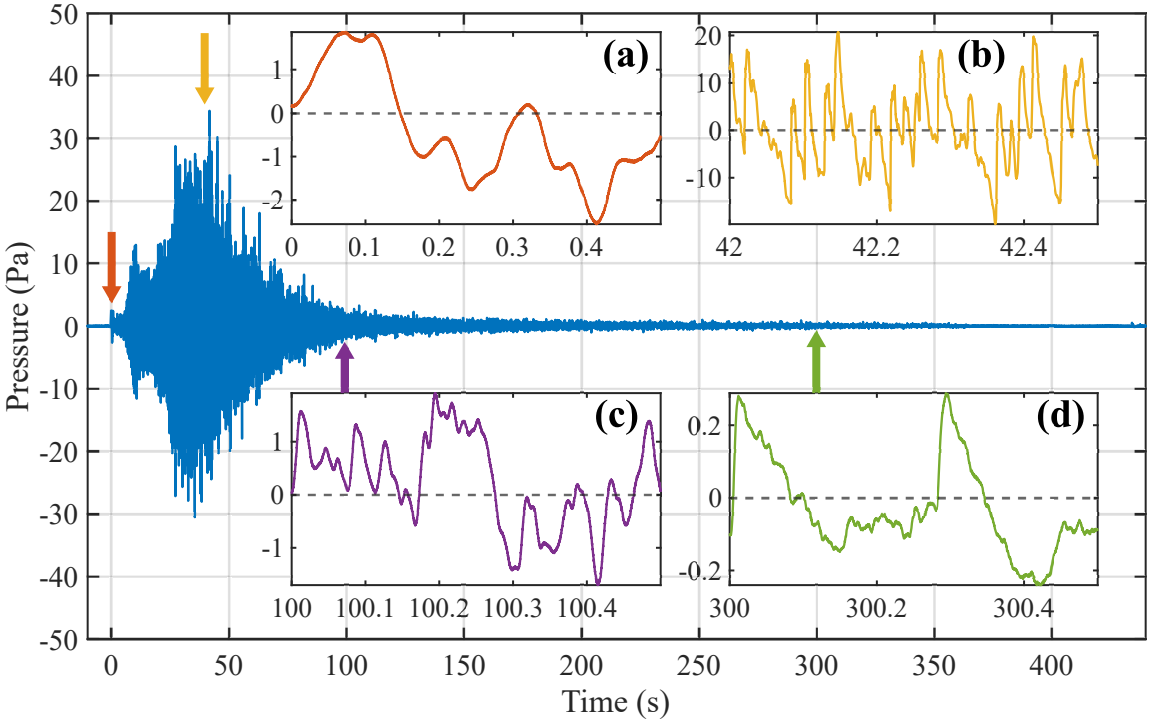

Figure 3.1 Representative waveform from RADARSAT Constellation launch. 0.5 s segments of the waveform are shown from three different time periods during the launch.(a) corresponds to the ignition overpressure, where a low frequency impulse is visible. (b) is from peak directivity where many acoustic shocks are visible. Acoustic shocks are still present in (c) and (d), with very pronounced shock structures present in (d).

corresponding to the waveform in Fig. 3.1. Block sizes used in computation of running OASPL and spectra are 1 second and 4 seconds, respectively. Spectra (a-d) correspond to the portions of the launch shown in Fig. 3.1(a-d), respectively. The measured running OASPL is reported in addition to the running OASPL corrected for geometric spreading caused by the movement of the vehicle away from the measurement location. When compared to the angle of the measurement relative to the rocket plume, it can be seen that the amplitude corrected OASPL flattens out as the angle relative to the rocket plume converges to $\pm 10°$. This convergence is due to the "cone of silence" phenomenon associated with jet noise near the exhaust axis.

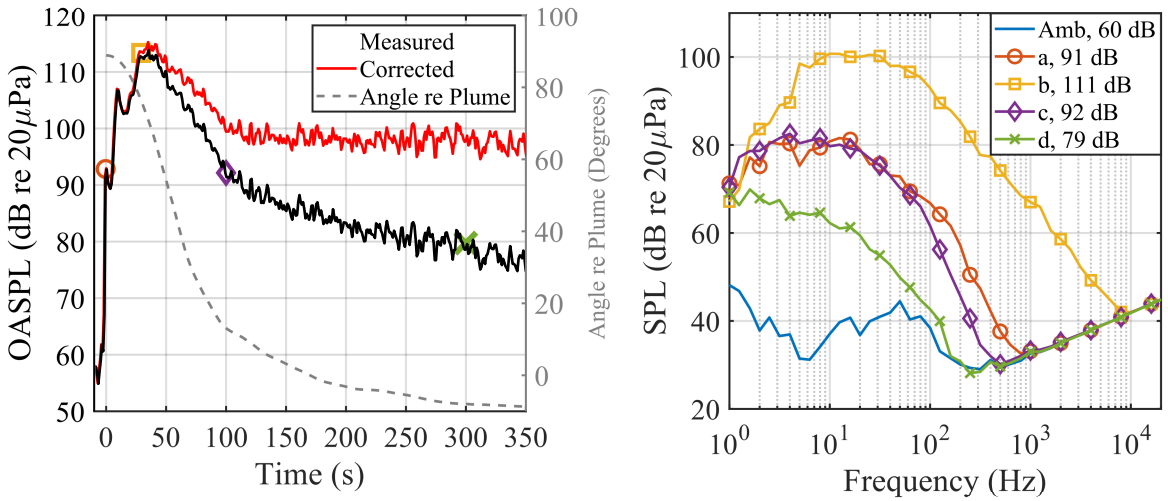

Figure 3.2 OASPL is plotted as measured and corrected for geometric spreading. Approximate angle relative to the rear end of the rocket is shown. Spectra are shown for time windows around times of the launch defined in Fig. 3.1. OASPLs for each spectrum are reported in the legend.

The spectra in Fig. 3.2 match what is qualitatively observable in the waveforms in Fig. 3.1. Spectra from (a) and (b) closely match, with the spectrum of (b) (peak directivity) containing the most high frequency content. The peak frequency in this region is about 30 Hz. Even in the late launch phase, 300 s into the launch where the rocket is greater than 64 km from the measurement site, the bandwidth of the measurement is over 100 Hz. The relatively high noise floor seen in these spectra is due to the higher noise floor associated with the low-frequency capable measurement hardware used and is compounded in the one-third octave spectra. Even so, at later times in the launch (such as that shown by Fig. 3.1(d)), the impact of filtering out the noise floor affects OASPL values by less than 0.01 dB. A method of dynamically filtering the instrumentation noise from the measured data, such as that proposed by Cook *et al.* [21], would be applicable if noise floor corruption were significant.

3.0.2 Comparison with Other Measurements and Models

Directivity

As mentioned previously, historical sources have shown variation between directivities of rockets fired in a static environment as opposed to launched vehicles. Cole *et al.* [6] observed peak radiation for launched vehicles to fall within the 70° to 80° range on average, while static peak radiation angles tended to fall within the 50° to 60° range. James *et al.* [15] showed a peak radiation angle of 60° to 65° for horizontally (static) fired RSRM. In comparison, Fig. 3.3 shows the average directivity of the Falcon 9 rocket across all measurements. A mean curve is shown with shaded region corresponding to one standard deviation from the mean. The median for this dataset is consistently within ± 1 dB of the mean. All OASPL curves were amplitude adjusted for spherical spreading to a common distance to allow for more direct comparison. These data show an average peak radiation angle of about 64°.

With regards to a predicted directivity, a convective Mach number of $M_{co} \approx 2.81$ would suggest a peak radiation angle of 69° given the relationship

$$\theta_{pk} = \cos^{-1}\left(\frac{1}{M_{co}}\right) \tag{3.1}$$

This is similar to findings for launch vehicles from Cole *et al.* [6] and the assumed peak directivity angle used by McInerny [7] but is not congruent with the measured directivity.

One possible explanation for this discrepancy is that the vehicle is moving while being measured. Considering that the rocket is moving with regard to the atmosphere surrounding the plume, the standard formulation of the Oertel convective Mach number using the ambient and plume parameters alone leaves out any consideration for vehicle movement. The convective Mach number attempts to describe the relative velocity at which turbulent structures in the mixing layer are convected downstream [3]. Since the mixing layer is caused by the mixing of the high

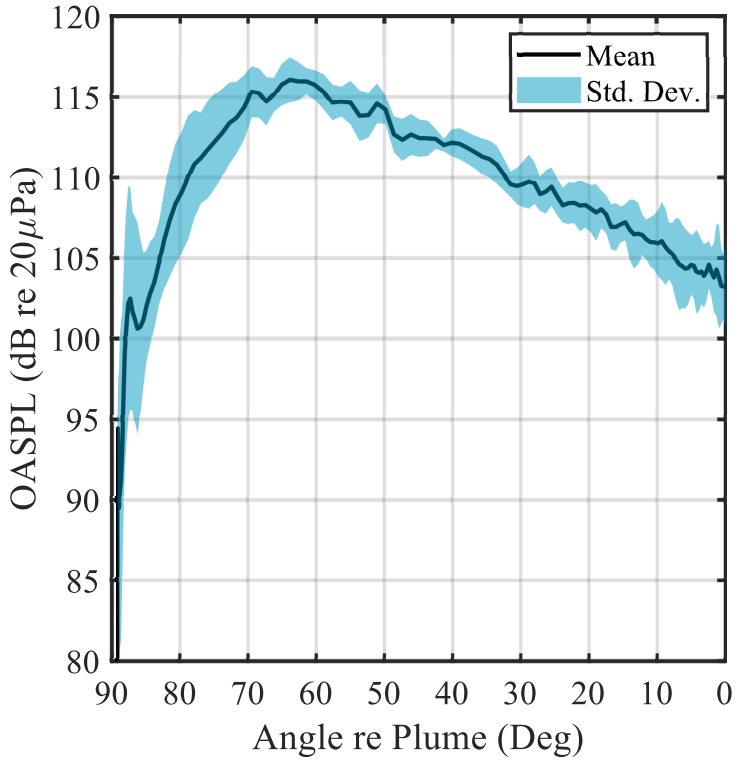

Figure 3.3 Mean OASPL across all measurements as a function of angle relative to the rocket plume, corrected for amplitude to a common distance of 6 km. The shaded region cooresponds to one standard deviation from the mean. While some variation is present, the mean peak directivity angle falls within the 60° to 70° range.

speed rocket exhaust and "static" atmosphere, an alteration of this static condition (such as by a moving rocket) may alter the properties of the mixing layer, the resulting convection, ultimately reducing the effective convective Mach number. This reduction would lead to a directivity shift towards the exhaust axis, as suggested by Ribner [22] and Sutherland [10].

Considering added velocity of the vehicle with respect to the calculated convective Mach number may provide a more accurate prediction of the peak radiation angle. While there are likely many methods of accounting for this, a simple example will be considered. The approximate vehicle speed at the measured peak level is M_v=0.55 relative to a sound speed of 340 m/s leading to an effective convective Mach number of approximately$M_{co} \approx 2.26$ as shown

in Eq. 3.2. This adjusted value results in a predicted peak radiation angle of 64° . This angle closer to the measured peak radiation angle of 64°.

$$M_{co,eff} = \frac{U_j + \frac{1}{2}c_j}{c_j + c_a} - M_v \tag{3.2}$$

I wish to note that the Oertel convective Mach number itself is an empirically derived number which has been found by Greska *et al.* [13] to relate to peak OASPL. In deriving this effective convective Mach number I acknowledge the empirical nature of this number and suggest this formulation to reflect observations made of launched vehicles. While the results are promising in context of the measured Falcon 9 directivity, additional studies and measurements are requisite to ratify its usefulness.

This predictive model using the convective Mach number is in contrast to a model used by McInerny [23], who utilizes a simpler model based on the speed of sound in the plume and the speed of sound in the surrounding atmosphere, as shown in Eq. 3.3.

$$\theta_{pk} = \cos^{-1}\left(\frac{c_a}{0.7c_e}\right) \tag{3.3}$$

Using this model, the predicted peak radiation angle is 58°. This does not agree well with either the previous convective Mach number model or the measured angle, but rather reflects earlier findings of Cole *et al.* [6] for static rockets. While this model is accurate according to Cole *et al.* [6] and other historical studies, it is incompatible with more modern measurements such as those presented in this paper.

Greska *et al.* [13] also uses a similar model, but instead assumes that the convection velocity is equivalent to 0.7 U_j. The predicted angle as given by Eq. 3.4 is 81° , far from McInerny's prediction and inconsistent with the measurements in this study.

$$\theta_{pk} = \cos^{-1}\left(\frac{c_a}{U_c}\right) = \cos^{-1}\left(\frac{c_a}{0.7U_j}\right) \tag{3.4}$$

Comparing these three methods of predicting the angle of peak radiation, the model that appears to be most reasonable in this study is that given by the effective Oertel convective Mach number from Eq. 3.1 and Eq. 3.2.

While the peak radiation angle is important, so also is the spread of the peak radiation region. The measured 3 dB down directivity peak for the Falcon 9 has an angular spread of about 25° on average. This is smaller than the 30° spread shown by Kenny *et al.* [14] for a horizontally fired RSRM and the 35° spread shown by Sutherland [10] for a launched Saturn I rocket (comparable in scale/thrust to the Falcon 9). In comparison to a directivity model proposed by Sutherland [10], the Falcon 9 directivity peak is significantly smaller, with Sutherland's model having a 3 dB down angular spread of 56°. While the variation in angular spread is evident, no reason for this variability is presented.

Overall Sound Power

With directivity established, the rocket sound power can be estimated. Using the measured directivity, the overall sound power level (OAPWL) for the Falcon 9 rocket is estimated to be 196 dB re 10 pW. This sound power estimation includes only the rear hemisphere surrounding the rocket (angles between 0° and 90° relative to the plume), however, due to the directivity associated with the rocket it is assumed that any contributions to the sound power from the front half of the rocket will be insignificant. This assumption is further shown to be reasonable by Matoza *et al.* [24].

In comparison with models, a 0.5% mechanical to acoustic power efficiency has been generally accepted for large rockets by Eldred [11], Guest [12], Sutherland [10], and others. Based on the rocket parameters in Table 2.3, the rocket mechanical power is expected to be 11.8 GW based on

the formulation for mechanical power being

$$W_{\text{mech}} = \frac{1}{2}\text{Th}\, U_e, \tag{3.5}$$

where W_{mech} is the mechanical power, Th is the vehicle thurst, and U_e is the exit velocity of the rocket. Assuming a 0.5% radiation efficiency, this would predict an overall sound power level of 198 dB re 10 pW. This prediction falls remarkably close to the measured sound power found earlier. While there is certainly room for error in these sound power calculations, this suggests that a 0.5% radiation efficiency for large rockets is reasonable as Guest [12] and Sutherland [10] have noted. If we assume that the estimated 196 dB sound power level is correct, however, we fund a predicted efficiency of 0.34%. This is close to the 0.5% prediction, albeit lower, showing that Eldred's [11] conservative 1% efficiency bound appears to be quite high.

Maximum Overall Level

The maximum OASPL in the direction of maximum radiation can be estimated based on known rocket acoustic parameters. McInerny [7] proposed a model of OASPL in the direction of maximum radiation based on sound power and an assumed directivity factor. This formulation is given as

$$\begin{aligned} \text{OASPL}_{\text{max}} &= \text{OAPWL} - 10\log 10(4\pi r^2) + Q_{textmax} \\ &= 10\log_1 0\left(\frac{\eta W_m}{10^{-12}\text{watts}}\right) - 10\log_{10}(4\pi r^2) + 10\log_{10} Q(\theta_{pk}) \end{aligned} \tag{3.6}$$

where η is the acoustic efficiency, W_m is the mechanical power, r is the radial distance from the source, and $10\log_{10} Q(\theta_{pk}) = Q_{\text{max}}$ is the directivity factor. The maximum directivity factor itself is a measure of the directionality of the source. What it represents is the relative "peak" of the maximum radiation lobe versus a monopole radiatin the same sound power. An acoutic monopole radiates sound out equally in every direction; it is totally symmetric source. If we were to take the OASPL of a directional source at the direction of maximum radiation, and subtract

from it the OASPL from a monopole of the same power output, this would be the maximum directivity factor $Q_{\max}$.

For a monopole source that radiates sound equally in every direction (omnidirectionally), the time-averaged sound power is given by

$$\bar{W} = S\bar{I} = 4\pi r^2 \bar{I} \tag{3.7}$$

where S is the area over the "sphere" of measurement and $\bar{I}$ is the time-averaged intensity. If we are sufficiently far from the source, we can make a plane wave assumption with regards to intensity, which yields

$$\bar{I} \approx \frac{\bar{p}^2}{\rho c}. \tag{3.8}$$

So, we relate the OASPL back to the OAPWL as

$$\begin{aligned} \text{OASPL}_{\text{monopole}} &= 10\log_{10}\left(\frac{\bar{p}^2}{p_{\text{ref}}^2}\right) \\ &\approx 10\log_{10}\left(\frac{\bar{I}}{I_{\text{ref}}}\right) \\ &= 10\log_{10}\left(\frac{\bar{W}}{4\pi r^2 I_{\text{ref}}}\right) \\ &= 10\log_{10}\left(\frac{\bar{W}}{W_{\text{ref}}}\right) - 10\log_{10}(4\pi r^2) \\ &= \text{OAPWL} - 10\log_{10}(4\pi r^2) \end{aligned} \tag{3.9}$$

Therefore, the maximum directivity factor for a source with a maximum OASPL at a distance r from the source is given as

$$\begin{aligned} Q_{\max} &= \text{OASPL}_{\max} - \text{OASPL}_{\text{monopole}} \\ &= \text{OASPL}_{\max} - \text{OAPWL} + 10\log_{10}(4\pi r^2). \end{aligned} \tag{3.10}$$

In her analyses, McInerny [7] indicated a range of 5 to 8 dB for $Q_{\max}$, but settled on 8 dB using data from Cole et al. [6]. Using this maximum directivity factor and assuming a radiation efficiency of 0.5%, $\text{OASPL}_{\max}$ is calculated to be 145 dB at a distance of 100 $D_{e,\text{equiv.}}$. This is

only 2 dB higher than the measured value scaled to the same distance of 143 dB, showing great promise for this simple, power-based model.

Greska *et al.* [13] proposed a relationship between the maximum OASPL in the direction of maximum radiation at 100 rocket exit diameters (D_e) and a convective Mach number. This convective Mach number, referred to as the Oertel convective Mach number (M_{co}), is the arithmetic average of two other convective Mach numbers given by Oertel and Patz [3] in Eqs. 1.2 and 1.3. This convective Mach number is formulated as Eq. 3.11, where U_j is the fully expanded jet velocity at the exit, c_j is the speed of sound at the exit for the fully expanded condition, and c_a is the speed of sound in the surrounding atmosphere.

$$M_{co} = \frac{1}{2}(M_c + M_c') = \frac{U_j + \frac{1}{2}c_j}{c_j + c_a} \tag{3.11}$$

Using the approximate fully-expanded parameters for the Falcon 9, an Oertel convective Mach number is found for the Falcon 9 to be $M_{co} \approx 3.00$ with an average peak level of 143 dB across all measurements. This is plotted along with data and curves proposed by Greska *et al.* [13] in Fig. 3.4. In addition, a point has been added for a Space Shuttle solid rocket booster measurement with a computed convective Mach number of $M_{co} \approx 2.30$ and a peak OASPL at 100 $D_{e,\text{equiv}}$ of 142 dB from James *et al.* [15] Additionally, the Falcon 9 levels are plotted with an effective convective Mach number ($M_{co} - M_v$). This effective number will be discussed in greater detail in context of directivity.

The fitted curve proposed by Greska *et al.* [13] seems to predict peak OASPL well, especially at convective Mach numbers below 1.2. For larger rockets, the model overestimates the estimated OASPL by about 2 dB on average for the Falcon 9 and 2 dB for the RSRM measured by Kenny *et al.* [14].

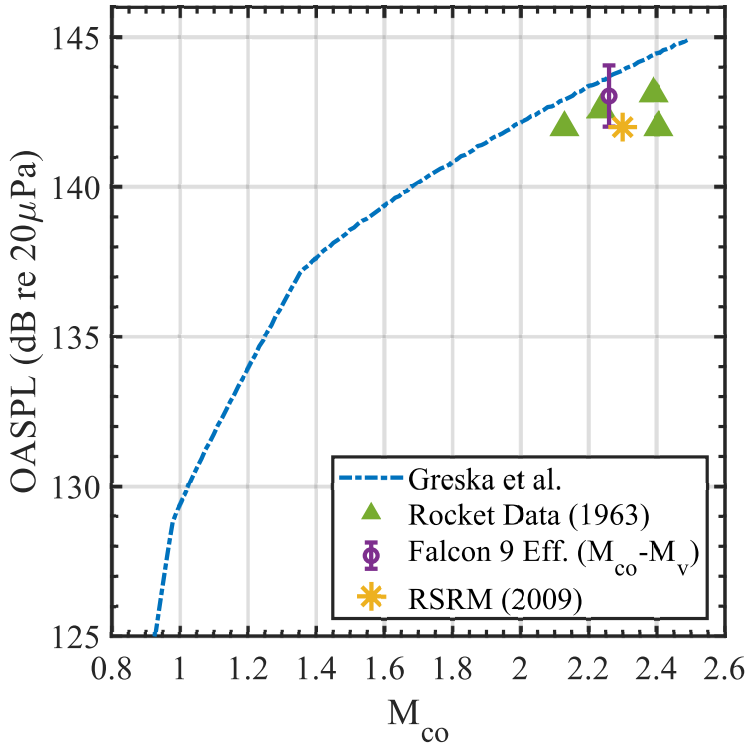

Figure 3.4 Data and curve given by Greska *et al.* Additional data points (RSRM and Falcon 9) are also shown.

3.1 Conclusions

In conclusion, measurements of the Falcon 9 rocket have provided both important information about rocket source characteristics, and have validated simple models for the prediction of rocket noise. Using an effective convective Mach number, the angle of maximum radiation is predicted to be 64°, which is what is shown from the measurements. By integrating the measured directivity, the sound power is estimated to be 196 dB re 10 pW, a mere 1 dB lower than what is calcualated from thrust, assuming an efficiency of 0.5% from the literature. Furthermore, two methods of calculating $\text{OASPL}_{\text{max}}$ in the maximum radiation direction produce predictions accurate to within 2 dB of the scaled measurement.

These simple models, based on a handful of rocket parameters accurately predict or approx-

imate three key acoustic properties of a rocket. The relevance of such models would be even more impactful if they hold for other jets, such as those found in military aircraft. Validation of these models for other jets will be the subject of future work. Other future work could investigate more source characteristics, such as frequency models beyond what was shown in Mathews et al [2]. In addition, ray tracing could be utilized to provide more accurate propagation modeling.

References

[1] L. T. Mathews, K. L. Gee, G. W. Hart, R. D. Rasband, D. J. Novakovich, F. I. Irrarazabal, A. B. Vaughn, and P. Nelson, "Comparative analysis of noise from three Falcon 9 launches," J. Acoust. Soc. Korea **39**, 322 (2020).

[2] L. T. Mathews, K. L. Gee, and G. W. Hart, "Characterization of Falcon 9 launch vehicle noise from far-field measurements," The Journal of the Acoustical Society of America **150**, 620–633 (2021).

[3] H. Oertel, "Measured Velocity Fluctuations Inside the Mixing Layer of a Supersonic Jet," Recent Contributions to Fluid Mechanics pp. 170–179 (1982).

[4] J. N. Cole and C. E. Thomas, "Far Field Noise and Vibration Levels Produced During the Saturn SA-1 Launch," techreport 61-607, Aeronautical Systems Division, Air Force Systems Command, United States Air Force (1961) .

[5] G. J. Putnicki, *Environmental Noise Assessment S.T.S.-1 Columbia Launch*, No. 2299 in *Twelfth Space Simulation Conference* (National Aeronautics and Space Administration, 1982), pp. 193–208.

[6] J. N. Cole, H. E. V. Gierke, and K. M. Eldred, "Noise Radiation From Fourteen Types of Rockets in the 1,000 to 130,000 Pounds Thrust Range," techreport 57-354, Wright Air Develoment Center (1957) .

[7] S. A. McInerny, "Launch Vehicle Acoustics Part 1: Overall Levels and Spectral Characteristics," Journal of Aircraft **33**, 511–517 (1996).

[8] W. H. Mayes, W. E. Lanford, and H. H. Hubbard, "Near-Field and Far-Field Noise Surveys of Solid-Fueld Rocket Engines for a Range of Nozzle Exit Pressures," techreport D-21, Langley Research Center, National Aeronautics and Space Administration (1959) .

[9] R. C. Potter and M. J. Crocker, "Acoustic Prediction Methods for Rocket Engines, Including the Effects of Clustered Engines and Deflected Exhaust Flow," techreport CR-566, George C. Marshalkl Space Flight Center, National Aeronautics and Space Administration (1966) .

[10] L. C. Sutherland, "Progress and Problems in Rocket Noise Prediction for Ground Facilities," 15th AIAA Aeroacoustics Conference (1993).

[11] K. M. Eldred, "Acoustic Loads Generated by the Propulsion System," techreport SP-8072, National Aeronautics and Space Administration (1971) .

[12] S. H. Guest, "Acoustic Efficiency Trends for High Thrust Boosters," techreport TN D-1999, George C. Marshall Space Flight Center, National Aeronautics and Space Administration (1964) .

[13] B. Greska, A. Krothapalli, W. C. Horne, and N. Burnside, *14th AIAA/CEAS Aeroacoustics Conference (29th AIAA Aeroacoustics Conference)* (2008), No. AIAA 2008-3026.

[14] R. J. Kenny, C. Hobbs, K. Plotkin, and D. Pilkey, *15th AIAA/CEAS Aeroacoustics Conference (30th AIAA Aeroacoustics Conference)* (2009), No. AIAA 2009-3161.

[15] M. M. James, A. R. Salton, K. L. Gee, T. B. Nielsen, S. A. McInerny, and R. J. Kenny, "Modificaiton of directivity cuerves for a rocket noise model," Proceedings of Meetings on Acoustics 18 (2012).

[16] S. A. McInerny, J. K. Francine, B. S. Stewart, and P. H. Thorson, "The influence of low-frequency instrumentation response on rocket noise metrics," The Journal of the Acoustical Society of America **102**, 2780–2785 (1997).

[17] K. L. Gee, D. J. Novakovich, L. T. Mathews, M. C. Anderson, and R. D. Rasband, "Development of a Weather-Robust Ground-BasedSystem for Sonic Boom Measurements," Technical Report No. NASA/CR-2020-5001870, National Aeronautics and Space Administration, Langley Research Center (2020) .

[18] K. L. Gee, D. J. Novakovich, L. T. Mathews, M. C. Anderson, and R. D. Rasband, "Development of a Weather-Robust Ground-Based System for Sonic Boom Measurements," Technical Report No. CR-2020-5001870, National Aeronautics and Space Administration (2020) .

[19] S. A. McInerny and S. M. Ölçmen, "High-intensity rocket noise: Nonlinear propagation, atmospheric absorption, and characterization," The Journal of the Acoustical Society of America **117**, 578–591 (2005).

[20] R. S. Ryan, J. H. Jones, S. H. Guest, H. G. Struck, M. H. Rheinfurth, and V. S. Verderaime, "Propulsion System Ignition Overpressure for the Space Shuttle," techreport NASA TM-82458, George C. Marshall Space Flight Center, National Aeronautics and Space Administration (1981) .

[21] M. R. Cook, K. L. Gee, M. L. Transtrum, S. Lympany, and M. Calton (unpublished).

[22] H. S. Ribner, "The Generation of Sound by Turbulent Jets," Adv. Appl. Mech. **8**, 103–182 (1964).

[23] S. A. McInerny, *AIAA 13th Aeroacoustics Conference* (1990), No. AIAA-90-3981.

[24] R. S. Matoza, D. Fee, T. B. Nielsen, K. L. Gee, and D. E. Ogden, "Aeroacoustics of volcanic jets: Acoustic power estimationand jet velocity dependence," Journal of Geophysical Research: Solid Earth **118**, 6269–6284 (2013).

Index